PROCEEDINGS OF SCIENCE

Propagation and acceleration of charged particles in astrophysical environments: an introduction

Germán Lugones*
Universidade Federal do ABC - Brazil
E-mail: german.lugones@ufabc.edu.br

In this review we present an introduction to some of the physics underlying the complex motion of charged particles in astrophysical environments. We study the equation of motion of charged particles in several contexts and present the basic mechanisms that allow to accelerate these particle to high energies.

4th School on Cosmic Rays and Astrophysics,
August 25- September 04, 2010
São Paulo, Brazil

*Speaker.

PoS(CRA School)029

1. Introduction

One of the preeminent puzzles in modern astrophysics concerns the nature and origin of cosmic rays. These particles arrive at the top of the Earth's atmosphere with energies extending from $\sim 10^9$ eV up to $\sim 10^{20}$ eV. There are also particles with less than 10^9 eV, but their spectrum is not well known because their flux is strongly reduced by the effect of the solar wind. Important information about cosmic rays come from the observation of the energy distribution of the particles. Let $N(E)dE$ be the number of cosmic rays in the energy interval dE. The observed energy spectrum $N(E)$ behaves as a power law, $N(E) \sim E^{-\gamma}$, where γ is:

$$\begin{aligned} \gamma &= 2.7 \quad \text{for} \quad 10^9\text{eV} < E < E_{knee}, \\ \gamma &= 3.0 \quad \text{for} \quad E_{knee} < E < E_{ankle}, \\ \gamma &= 2.7 \quad \text{for} \quad E_{ankle} < E < E_{GZK}, \end{aligned}$$

being $E_{knee} \approx 10^{16}$ eV, $E_{ankle} \approx 4 \times 10^{18}$ eV and $E_{GZK} \approx 6 \times 10^{19}$ eV. Extensive air shower experiments (e.g. AUGER, HiRes) show that above E_{GZK} the spectrum falls off. This is interpreted as a consequence of the energy loss (pion production) of cosmic rays as they interact with photons of the cosmic microwave background.

The charged primary particles of cosmic rays consist of $\sim 89\%$ of protons, $\sim 10\%$ of heavier nuclei (mainly alpha particles), and $\sim 1\%$ electrons. There are also very small proportions of positrons, antiprotons, muons, pions and kaons generated by interactions of the primary particles with the interstellar gas. Additionally, there are γ-rays and neutrinos and antineutrinos.

An essential ingredient for the acceleration and propagation of cosmic rays is the cosmic magnetic field. Magnetic fields are widely encountered in astrophysical environments: planets, stars, the interstellar medium, galaxies, the intergalactic medium and the large scale Universe are all permeated by them. In contrast, electric fields are not so easy to find. Since most of the matter in the Universe is in the plasma state, electric fields are screened on scales of the order of the Debye length. Therefore, electric fields can be encountered on some compact regions such as the polar caps of neutron stars or reconnection zones in stellar coronae or accretion disks, but are not expected on large scales.

Most cosmic rays are produced and accelerated within the galaxy and then propagate through galactic medium before arriving to the Earth. However, the fact that some particles attain $E \sim E_{GZK}$ indicates that at least part of them could be of extragalactic origin, since the galactic magnetic field cannot retain them. Actually, the hardening of the spectrum above E_{ankle} is indicative of an extragalactic origin of these particles.

While our knowledge of the galactic and extragalactic magnetic fields is still far from complete, there has been a significant progress in the last years and a large wealth of information is expected in the near future with the advent of the SKA array (see [1]). In recent years the magnetic field of several galaxies has been observed showing that fields with a well-ordered spiral structure exist in many types of galaxies (see e.g. [2, 3]). In general, interstellar magnetic fields are stronger in massive spiral arms and in nuclear starburst regions. For edge-on galaxies, radio polarization measurements show the existence of magnetic halos extending few kiloparsecs above and below the galactic disks. Inside the Milky Way, the diffuse interstellar medium, molecular clouds, and HII regions, are all permeated by magnetic fields. Rotation measures and dispersion measures of

pulsars show that the Galactic large-scale magnetic fields are aligned with the spiral arms. There are multiple reversals of the field direction as one moves from the innermost arm to the outer arm. The average strength of the local regular field is in the range of few μG. On smaller scales, the fields are enhanced when interstellar gas contracts to form a cloud, i.e. the observed field strength increases with gas density. Additionally, there is a turbulent field whose amplitude is thought to be larger than the regular one, with a coherence length of roughly 100 parsecs.

The propagation of charged cosmic rays along such intricate magnetic fields results in complex trajectories that must be studied numerically. In this review we shall focus on some basic physical mechanisms underlying the complex motion of charged particles in astrophysical environments in order to contribute to the understanding of the most recent results presented in other chapters of this book.

2. Acceleration in gravitational and electric fields

• *Gravitational acceleration.* The velocity acquired by a cosmic ray falling from infinity onto a stellar object of mass M and radius R is:

$$v = \sqrt{\frac{2GM}{R}}. \tag{2.1}$$

Thus, the compactness M/R of the stellar object determines the maximum velocity to which the particle may be accelerated in the gravitational field. For white dwarf stars ($R \sim 10^4$ km, $M \sim 1M_{\odot}$) the maximum velocity is $v_{max} \approx 0.025c$ corresponding to a Lorentz factor $\gamma_{max} \approx 1.0003$, which is too small for producing relativistic particles. For neutron stars ($R \sim 10$ km, $M \sim 1.5-2M_{\odot}$) we find $v_{max} \sim c/2$, and $\gamma_{max} \sim 1.2$. This result is more interesting but still far from the large values required for cosmic rays.

• *Electric fields.* For some compact objects, the time variation of the magnetic field could lead to the generation of large electromotive forces. Let us consider the Faraday's law $\varepsilon = -d\phi/dt$, where $\varepsilon = \oint_C \mathbf{E}\cdot d\mathbf{l}$ is the electromotive force generated by the variation of the magnetic field and $\phi = \int_S \mathbf{B}\cdot d\mathbf{A}$ is the magnetic flux across a surface S inside a closed curve C. Thus:

$$\oint_C \mathbf{E}\cdot d\mathbf{l} = -\frac{d}{dt}\int_S \mathbf{B}\cdot d\mathbf{A}. \tag{2.2}$$

For the flux variation over a surface closed by a circular region with radius R we obtain $\phi = B\pi R^2$. After one cycle around such region a particle of charge q gains an energy:

$$E = q\varepsilon = q\pi R^2 \frac{dB}{dt} \sim \frac{q\pi BR^2}{\tau} \tag{2.3}$$

where τ is some typical timescale for the variation of the magnetic field.

In the case of the Sun, turbulent motions of the electron-proton plasma produce currents that generate magnetic fields. The eventual further decay of these fields may give rise to electric fields that are able to accelerate the electrons and the protons. Let us consider a dark magnetized sunspot on the solar surface with a field $B \sim 2000$ G, radius $R \sim 10^4$ km, and a lifetime of one day. Using Eq. (2.3) we find that the energy gain is $E \approx 0.7$ GeV. Although the details on how this energy

is transferred to the gas particles are still not fully understood, and other acceleration mechanisms such as Fermi process or magnetic reconnection may be also occurring on the solar surface, this simple estimate shows that at least there is sufficient energy in sunspots to accelerate particles to high energies. Actually, cosmic rays up to 10^{11} eV have been observed coming from the Sun.

Similar arguments can be applied to the case of pulsars. They are very compact objects ($R \approx 10$ km) with surface magnetic fields of $\sim 10^{12} - 10^{14}$ G, that rotate with periods as fast as $0.03s$. A more careful calculation than the one given above leads to the following result:

$$E \approx \frac{qB\Omega^2 R^3}{2}, \tag{2.4}$$

where Ω is the rotation frequency (more details about this formula can be found in [7, 9, 8]). With Eq. (2.4) we can show that varying magnetic fields at the magnetosphere of pulsars are able to accelerate particles to at most 10^{15} eV, which is not sufficient to produce ultra-high energy cosmic rays (which have energies $> 10^{18}$ eV). However, the possibility of accelerating these ultra-high energy cosmic rays in pulsars still deserves more study. For example, some neutron stars called *magnetars* are believed to have fields of 10^{15} G although unfortunately they have long rotation periods (some seconds). But, very young neutron stars are expected to have at the same time a large field and a short rotation period (near milliseconds) and thus we can obtain $E \approx 4 \times 10^{19}$ eV for protons, and $E \approx 10^{21}$ eV for iron nuclei. Thus, it seems that neutron stars are viable accelerators for high energy cosmic rays but theoretical models should be worked in detail.

3. Motion of charged particles in uniform magnetic fields

In this section we shall show that to lowest order, charged particles perform a helical motion along the magnetic field lines. This is true within both a non-relativistic and a relativistic treatment. We also show that the kinetic energy of charged cosmic rays is conserved as they propagate trough 'non-moving' magnetic fields. Finally, we show some estimates about the trajectories of energetic charged particles in the galactic magnetic field.

3.1 Non-relativistic case.

The simplest case is $B =$ constant and $E = 0$. For this case the equation of motion is:

$$m\frac{d\mathbf{v}}{dt} = q\mathbf{v} \times \mathbf{B} \tag{3.1}$$

Taking $\mathbf{B} = B\hat{\mathbf{z}}$ we have:

$$m\frac{dv_x}{dt} = qv_yB, \tag{3.2}$$

$$m\frac{dv_y}{dt} = -qv_xB, \tag{3.3}$$

$$m\frac{dv_z}{dt} = 0. \tag{3.4}$$

The first two equations can be written as

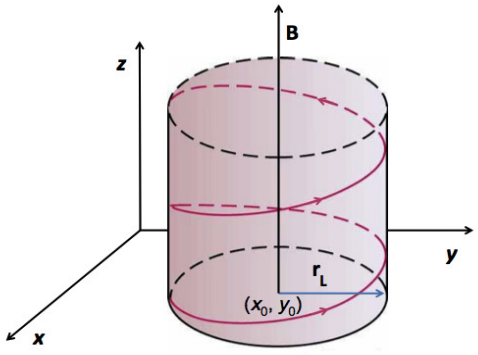

Figure 1: Helical motion of a charged particle in a uniform magnetic field. The motion is a combination of a uniform displacement along a magnetic field line and a circular motion around a field line (in a circle of radius r_L).

$$m\frac{d^2v_x}{dt^2} = -\left(\frac{qB}{m}\right)^2 v_x, \tag{3.5}$$

$$m\frac{d^2v_y}{dt^2} = -\left(\frac{qB}{m}\right)^2 v_y, \tag{3.6}$$

which describe a simple harmonic oscillator at the *cyclotron frequency* $\omega_c \equiv qB/m$. Thus, the solution of the equations of motion can be written as:

$$\frac{dx}{dt} \equiv v_x = v_\perp \sin(\omega_c t + \delta) \tag{3.7}$$

$$\frac{dy}{dt} \equiv v_y = v_\perp \cos(\omega_c t + \delta) \tag{3.8}$$

$$\frac{dz}{dt} \equiv v_z = v_\parallel \tag{3.9}$$

where δ is an arbitrary phase, $v_\perp$ is a positive constant denoting the speed in the plane perpendicular to **B**, and $v_\parallel$ is the constant speed in the direction parallel to **B**. Integrating the equations above we have:

$$x - x_0 = -r_L \cos(\omega_c t + \delta) \tag{3.10}$$

$$y - y_0 = r_L \sin(\omega_c t + \delta), \tag{3.11}$$

$$z - z_0 = v_\parallel t \tag{3.12}$$

where we have defined the *Larmor radius* (also known as gyration or cyclotron radius) as $r_L = v_\perp/|\omega_c|$, and x_0, y_0, y_0 are constants. In the xy-plane we have a circular orbit around a *guiding center* (x_0, y_0) with a radius r_L while in the z direction we have a uniform motion. Thus, the equations describe a helical motion of the charged particle along the z direction. For positive particles we have a left-handed motion and for negative particles a right-handed motion.

3.2 Relativistic case.

The equation of motion is now

$$\frac{d}{dt}(m\gamma\mathbf{v}) = q\mathbf{v}\times\mathbf{B}. \tag{3.13}$$

where γ is the Lorentz factor defined as $\gamma = (1-v^2)^{-1/2}$, with v in units of the speed of light c. If we dot both sides of the equation with $\mathbf{v}$ we have:

$$\mathbf{v}\cdot\frac{d}{dt}(m\gamma\mathbf{v}) = q\mathbf{v}\cdot(\mathbf{v}\times\mathbf{B}). \tag{3.14}$$

The right hand side of the equation is zero because $\mathbf{v}\perp(\mathbf{v}\times\mathbf{B})$. The left hand side can be written as follows:

$$\mathbf{v}\cdot\frac{d}{dt}(m\gamma\mathbf{v}) = m\gamma\mathbf{v}\cdot\frac{d\mathbf{v}}{dt} + m\mathbf{v}^2\frac{d\gamma}{dt} = \tag{3.15}$$

$$= \frac{1}{2}m\gamma\frac{d(\mathrm{v}^2)}{dt} + m\mathrm{v}^2\frac{d\gamma}{d(\mathrm{v}^2)}\frac{d(\mathrm{v}^2)}{dt} \tag{3.16}$$

$$= m\left(\frac{1}{2}\gamma + \mathrm{v}^2\frac{d\gamma}{d(\mathrm{v}^2)}\right)\frac{d(\mathrm{v}^2)}{dt} = 0. \tag{3.17}$$

Since the first factor of Eq. (3.17) is non-zero, we have $d(\mathrm{v}^2)/dt = 0$ and, therefore, $v^2 =$ constant and $\gamma =$ constant. Thus, the kinetic energy of the charged particle is not changed by the magnetic field:

$$E = m\gamma c^2 = \text{constant}. \tag{3.18}$$

Notice that this is true in a general non-uniform magnetic field, provided that the electric field is zero.

The solution of the equation of motion is straightforward. Since $\gamma =$ constant, Eq. (3.13) reads $m\gamma d\mathbf{v}/dt = q\mathbf{v}\times\mathbf{B}$ and therefore the particle's trajectory is described by Eqs. (3.10,3.11,3.12) but with a relativistic gyro-frequency and gyro-radius given by

$$\omega_c \equiv \frac{qB}{\gamma m}, \tag{3.19}$$

$$r_L \equiv \frac{v_\perp}{\omega_c} = \frac{\gamma m v_\perp}{|q|B} = \frac{\gamma m v_\perp}{qB} = \frac{p_\perp}{qB} = \frac{p\sin\theta}{qB} \tag{3.20}$$

where, p is the moment of the particle and the angle θ between p and the magnetic field is called *pitch angle*. Notice that the gyro-frequency is independent of energy in the non-relativistic case, but it is inversely proportional to the energy for relativistic particles.

Interesting conclusions can be obtained by comparing the radius of the galaxy, $r_G \approx 10$ kpc with the Larmor radius of a cosmic ray of energy E and charge Ze. Very high energy cosmic rays are almost undeflected as they move trough the galaxy; try for instance $Z = 1$, $E = 10^{19}$ eV and $B = 2\mu G$. Indeed, for $E/Z > 10^{18}$ eV, the trajectories of cosmic rays are not confined within the Galaxy, but for lower E/Z they remain trapped in the Milky Way for a long time. For $E/Z < 10^{17}$ eV they scatter off the turbulent magnetic field irregularities making a random walk. For $E/Z < 10^{14}$ eV the cosmic ray sky becomes completely isotropic due to this scattering.

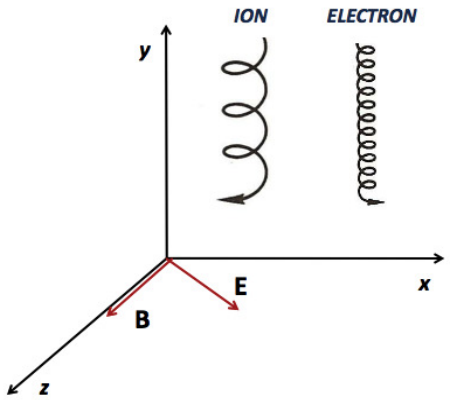

Figure 2: Motion of a charged particle in a constant electric and magnetic field. On the left it is shown the motion of a positively charged particle (e.g. an ion). On the upper half cycle of the orbit the particle gains energy due to the x component of the electric field; thus, $v_\perp$ and r_L increase. In the lower half cycle of the orbit the particle losses energy because it moves against E_x; thus, r_L decreases. The difference in r_L on the left and right hand sides of the orbit causes the drift v_E in the $-y$ direction. On the right of the figure it is shown the motion of a negatively charged particle (e.g. an electron). Now the particle gyrates in the opposite direction but also gains energy in the opposite direction. As a consequence a negative particle drifts in the same direction as a positive one. Notice that for simplicity we have not included in the plot the accelerated motion along the z direction.

4. Motion in non-uniform electromagnetic fields

For arbitrary non-uniform electromagnetic fields the problem becomes too complicated to be solved exactly. In general it is necessary to solve numerically the equation of motion

$$m\frac{d^2\mathbf{r}}{dt^2} = q(\mathbf{E}+\mathbf{v}\times\mathbf{B}), \tag{4.1}$$

for a charged particle in an arbitrary field configuration. Since this kind of analysis is out of the scope of the present review, we shall obtain some general conclusions about the effect of electric fields and then we shall focus on curvature and gradients of the magnetic field. Then, we discuss the magnetic mirror effect and finally we show some results of numerical simulations of charged particle propagation in the turbulent magnetic field around a shock front.

• *Drift motions.* Let us consider $B =$ constant along the z direction and $E =$ constant. Notice that we may choose $\mathbf{E}$ to be in the xz-plane by rotating the reference frame appropriately. Thus, the equation of motion $m\frac{d\mathbf{v}}{dt} = q(\mathbf{E}+\mathbf{v}\times\mathbf{B})$ reads:

$$\frac{dv_x}{dt} = \frac{q}{m}E_x + \omega_c v_y, \tag{4.2}$$

$$\frac{dv_y}{dt} = -\omega_c v_x, \tag{4.3}$$

$$\frac{dv_z}{dt} = \frac{q}{m}E_z. \tag{4.4}$$

Eq. (4.4) describes an acceleration of the particle along the direction of **B**. The solution of the transverse motion is:

$$\frac{dx}{dt} \equiv v_x = v_\perp \sin(\omega_c t + \delta), \tag{4.5}$$

$$\frac{dy}{dt} \equiv v_y = v_\perp \cos(\omega_c t + \delta) - \frac{E_x}{B}. \tag{4.6}$$

Therefore, the motion has the following properties: (a) there is an acceleration along **B** due to the z component of the electric field, (b) we have a circular Larmor gyration in the xy plane, (c) superimposed to the Larmor motion there is a *drift* of the guiding center in the y direction with a velocity $v_E = -E_x/B$. The resulting motion and a qualitative explanation of it are given in Fig. 2.

In general, it is easy to show that the drift velocity due to an electric field is:

$$\mathbf{v_E} = \frac{\mathbf{E}\times\mathbf{B}}{B^2}. \tag{4.7}$$

Notice that v_E is independent of the mass and the electric charge of the particle.

• *Curvature of field lines.* The expression for the drift velocity given above can be generalized to other forces by replacing **E** with $\mathbf{F}/q$, where **F** is a general force. The resulting drift of the guiding center is then,

$$\mathbf{v_F} = \frac{\mathbf{F}\times\mathbf{B}}{qB^2}. \tag{4.8}$$

Let us consider a magnetic field of constant strength ($|\mathbf{B}| = $ constant) but curved with a constant curvature radius r_C. The centrifugal force felt by the particle as it moves along the magnetic field lines originates a drift of the guiding center. The centrifugal force can be written as:

$$\mathbf{F}_C = \frac{mv_\parallel^2 \mathbf{r}_C}{\mathbf{r}_C^2} \tag{4.9}$$

where $v_\parallel$ denotes the velocity along the direction of **B**. Thus, the curvature drift is given by

$$\mathbf{v_C} = \frac{\mathbf{F}_C\times\mathbf{B}}{qB^2} = \frac{mv_\parallel^2}{qB^2}\frac{\mathbf{r}_C\times\mathbf{B}}{\mathbf{r}_C^2}, \tag{4.10}$$

resulting a motion that is perpendicular to both the curvature radius and the magnetic field.

• *Gradient of* **B**. Now we analyse a magnetic field that has a gradient along a direction that is perpendicular to the magnetic field lines ($\nabla|\mathbf{B}|\perp\mathbf{B}$). For simplicity we consider straight magnetic field lines in the z direction, as shown in Fig 3. Because of the gradient in $|\mathbf{B}|$ the Larmor radius is smaller at the top of the orbit than at the bottom of it. This causes a drift which has opposite directions for negatively and positively charged particles. An elementary calculation that is left to the reader shows that the drift velocity is given by:

$$\mathbf{v_{\nabla B}} = \frac{r_L v_\parallel^2}{2}\frac{\mathbf{B}\times\nabla|\mathbf{B}|}{B^2}, \tag{4.11}$$

i.e., charged particles drift along the x direction as shown in Fig. 3.

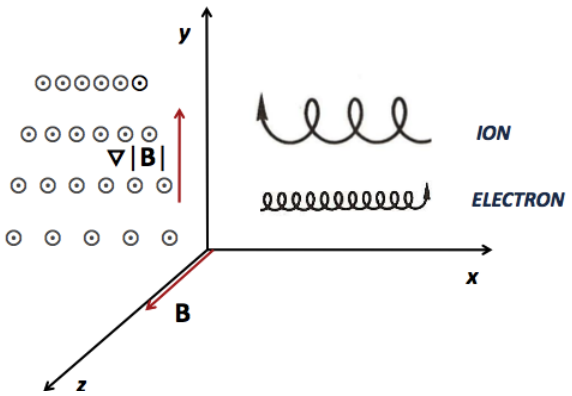

Figure 3: Drift motion due to a gradient of the magnetic field.

• *Magnetic mirror.* An effect that is of outstanding relevance for the understanding of cosmic ray acceleration is *magnetic mirroring*. Let us consider an axisymmetric magnetic field pointed primarily in the z direction and whose magnitude varies in the z direction. Since the magnetic field is divergence free, it will have x and y components as the lines approximate each other, and the field lines will look as shown in Figure 4.

Let us now consider a charged particle spiraling along the z direction (coming from the left of the plot). It is possible to show that for most spatially and temporally varying magnetic fields the magnetic moment of the particle

$$\mu \equiv \frac{\frac{1}{2}mv_{\perp}^2}{B}, \tag{4.12}$$

remains invariant as the particle moves (it is an *adiabatic invariant*). When the particle moves into the region with larger B, the velocity $v_{\perp}$ must increase in order to keep $\mu =$ constant. But the kinetic energy $E = \frac{1}{2}mv_{\parallel}^2 + \frac{1}{2}mv_{\perp}^2$ is also a constant. Thus, when $v_{\perp}$ increases, $v_{\parallel}$ must decrease. If B grows enough, $v_{\parallel}$ goes to zero as the particle moves and the particle is reflected back to the

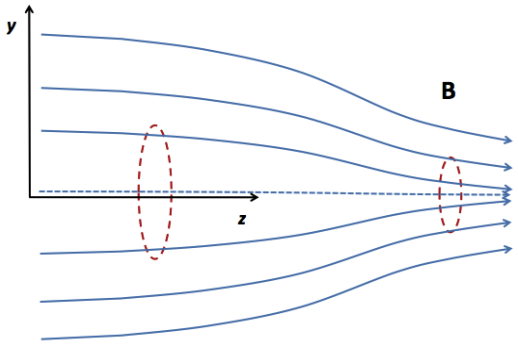

Figure 4: Magnetic mirroring.

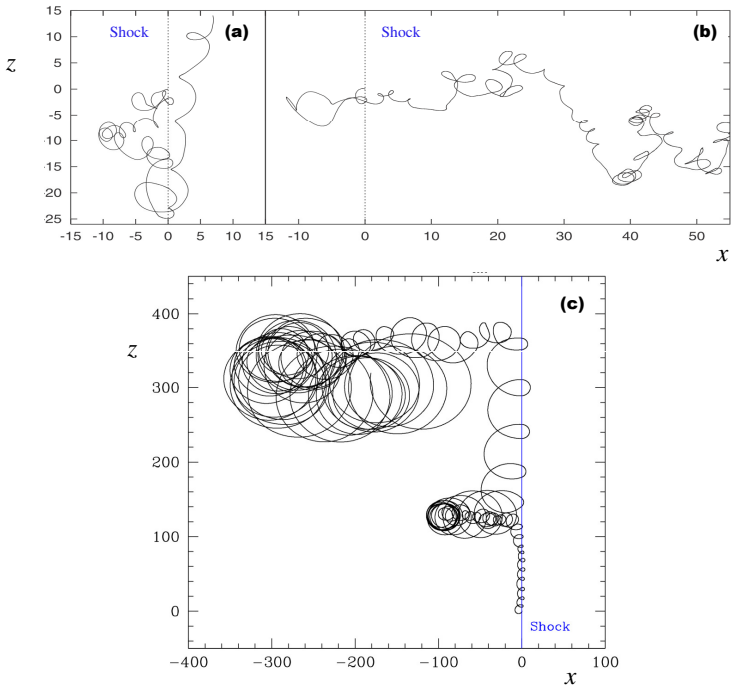

Figure 5: A portion of the trajectories of three charged particles that are accelerated from low to high energies due to magnetic inhomogeneities around three different shock discontinuities. Panels (a) and (b) were adapted from Ref. [10] and panel (c) from Ref. [11]. The results were obtained through Monte Carlo simulation of test-particles in relativistic magnetohydrodynamic shock waves.

region of smaller B.

• *Motion in complex magnetic fields.* As an example of the motion of charged particles in complex magnetic field configurations we shall briefly address particle acceleration at astrophysical shock waves. When encountering a collisionless shock, charged particles may be accelerated by means of two basic mechanisms. In the first-order Fermi acceleration mechanism (to be discussed below), particles stochastically diffuse back and forth across the shock front and gain energy by scattering from magnetic turbulence embedded in the converging flows. Alternatively, in magnetized flows, particles may also gain energy directly from the background motional electric field $\mathbf{E} = \mathbf{u} \times \mathbf{B}$ while they gyrate around the shock (here $\mathbf{u}$ is the velocity of the plasma). The latter process is given different names (e.g. Shock Drift Acceleration and Shock Surf Acceleration) depending on the barrier that reflects the particles back and forth. In Fig. 5 we show results obtained by the numerical integration of the particle equations of motion in the turbulent magnetic field near relativistic magnetohydrodynamic shock fronts [10, 11]. Typical drift motions described before can be identified in several directions.

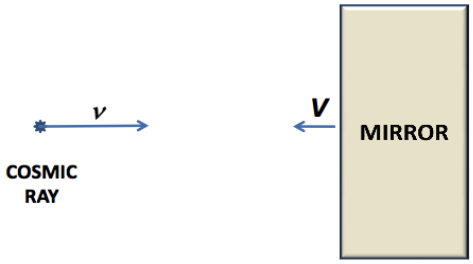

Figure 6: Collision of a charged particle with a magnetic mirror.

5. Collision of a cosmic ray with a magnetic mirror

In a previous section we showed that a static magnetic field cannot accelerate charged particles. However, the situation may be different for non-static magnetic fields. For simplicity, let us consider the *one-dimensional* collision of a cosmic ray of rest mass m with a moving magnetic mirror of mass M. In the observer's frame the velocities of the cosmic ray and the mirror are v and V respectively.

Thus, the initial four-momentum of the cosmic ray in the observer's frame is:

$$p_i^\mu = \begin{pmatrix} E/c \\ p \end{pmatrix} = \gamma(v) m \begin{pmatrix} c \\ v \end{pmatrix}. \tag{5.1}$$

In a reference frame fixed to the magnetic mirror we have $p_i^{'\mu} = \Lambda(V) p_i^\mu$ where $\Lambda(V)$ is a boost with velocity V. Thus,

$$p_i^{'\mu} = \Lambda(V) p_i^\mu = \gamma(V) \begin{pmatrix} 1 & V/c \\ V/c & 1 \end{pmatrix} \times \gamma(v) m \begin{pmatrix} c \\ v \end{pmatrix} = \gamma(V)\gamma(v) m \begin{pmatrix} c + \frac{vV}{c} \\ V + v \end{pmatrix} \tag{5.2}$$

being $\gamma(v) = [1 - v^2/c^2]^{-1/2}$ the Lorentz factor.

Now, we shall consider elastic collisions in the mirror's frame. In this case the particle's energy after the collision is the same as before the collision and the momentum is inverted. Therefore, the final momentum of the cosmic ray is:

$$p_f^{'\mu} = \gamma(V)\gamma(v) m \begin{pmatrix} c + \frac{vV}{c} \\ -V - v \end{pmatrix}. \tag{5.3}$$

Finally, we turn back to the observer's frame:

$$p_f^\mu = \Lambda(-V) p_f^{'\mu} = \gamma(V)^2 \gamma(v) m \begin{pmatrix} c + \frac{2vV}{c} + \frac{V^2}{c} \\ -v - 2V - \frac{V^2 v}{c} \end{pmatrix}. \tag{5.4}$$

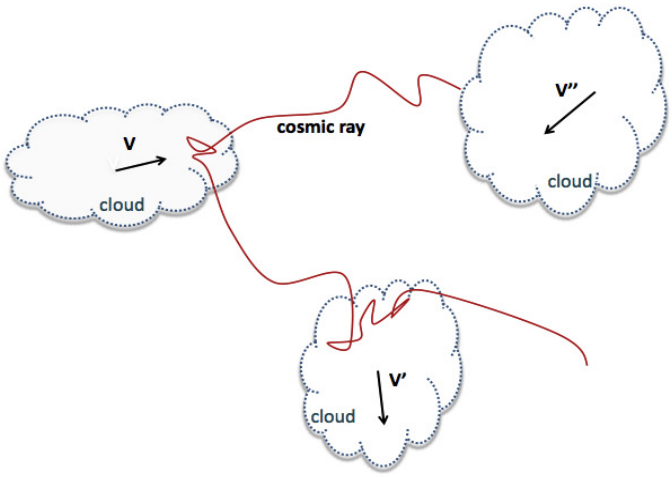

Figure 7: In the second order mechanism proposed by Fermi, cosmic rays collide stochastically with the magnetic field embedded in randomly moving interstellar clouds. Since head-on collisions are more probable than tail collisions, a cosmic ray gains kinetic energy after several reflections.

In the observer's frame, the ratio between the particle's energy after and before reflection is:

$$\frac{E_f}{E_i} = \frac{\gamma(V)^2\gamma(v)m\left(c+\frac{2vV}{c}+\frac{V^2}{c}\right)}{\gamma(v)mc} = \frac{\left(1+\frac{2vV}{c^2}+\frac{V^2}{c^2}\right)}{1-\frac{V^2}{c^2}}. \tag{5.5}$$

For $V \ll c$ we have

$$\frac{E_f}{E_i} = 1+\frac{2vV}{c^2}+\frac{2V^2}{c^2}+\mathscr{O}\left(\frac{V^3}{c^3}\right), \tag{5.6}$$

and then, the relative energy change is

$$\frac{\Delta E}{E} \equiv \frac{E_f - E_i}{E_i} = \frac{2vV}{c^2}+\frac{V^2}{c^2} \approx 2\frac{V}{c}+2\frac{V^2}{c^2}. \tag{5.7}$$

Since the first order term can be positive or negative we have:

$$\begin{array}{lccl} \text{for head-on collisions:} & \frac{\Delta E}{E} > 0 & \rightarrow & \text{energy gain,} \\ \text{for back collisions:} & \frac{\Delta E}{E} < 0 & \rightarrow & \text{energy loss.} \end{array} \tag{5.8}$$

6. Second order Fermi mechanism

One of the earliest theories on the acceleration of cosmic rays was proposed by Enrico Fermi [5] and became known as the *second order Fermi mechanism*. Although it is now clear that such a mechanism is too slow to obtain high particle energies in the known lifetime of cosmic rays in the galaxy, it is still the basis of much of the work on acceleration theory.

In this model, particles collide stochastically with many magnetic clouds in the interstellar medium. In a collision with a receding cloud the cosmic ray loses energy (the cloud velocity is $-V$). In a collision with an approaching cloud the CR gains energy (the cloud velocity is $+V$)

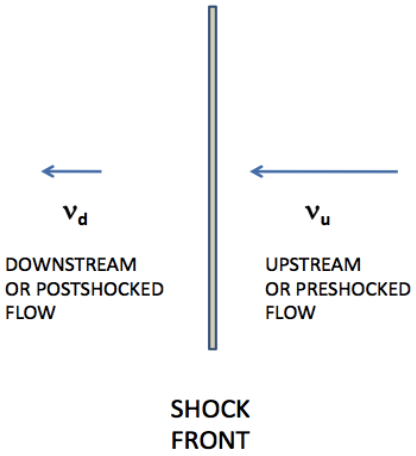

Figure 8: Sketch of a shock wave discontinuity showing the upstream and downstream flows.

Since clouds velocities are distributed randomly, we expect that if we calculate the average energy gain after several collisions, the first order term will vanish, leaving only second-order terms $\propto V^2/c^2$:

$$\frac{\Delta E}{E} \propto \frac{V^2}{c^2}. \tag{6.1}$$

That is, on average there is an energy gain. This occurs even in a completely random medium because head-on collisions are more probable than back collisions (when you drive a car in the rain, the amount of water hitting the front windshield is larger than the amount hitting the rear windshield). Unfortunately, the energy gain is only second order, which is not as efficient as the first order one. In the case of collisions with interstellar clouds it is now clear that such a mechanism is too slow to obtain high energy particles in the few million years that a cosmic ray stays in the galaxy. However, the main idea of the mechanism has a wide applicability, e.g. cosmic rays can collide with magnetic inhomogeneities on both sides of a shock front, or with small moving inhomogeneities in turbulent plasmas. In the next sections we shall concentrate on the interaction with shock fronts and we shall show that it leads to a much more efficient first order mechanism.

7. Shock waves

Shock phenomena are very frequent in astrophysical fluids. They span a large range of scales, including the bow shock caused by the Earth's magnetic field colliding with the solar wind, interplanetary shock waves when the solar wind collides with planetary magnetospheres, the termination shock in the ultra-relativistic wind from young pulsars, shocks surrounding supernova remnants due to the interaction of the expanding ejecta with the interstellar medium, shock waves in the jets of protostellar objects, microquasars, gamma ray bursts (GRBs) and active galactic nuclei (AGNs), and shock waves caused by galaxies colliding with each other.

From a hydrodynamic point of view, shock waves are surface discontinuities in the physical variables of a flow involving a flux of mass, momentum and energy through the surface, which are caused when a fluid moves supersonically into another one. In reality, the discontinuity is not infinitely steep but it has a finite thickness. However, we will not examine the complex physical phenomena that may occur inside the front. Instead, our scope is to solve the conservation laws across the shock front in order to derive a simple relationship between the velocities of the fluid on both sides of the discontinuity that will be useful for understanding the first order Fermi acceleration mechanism.

For simplicity we shall assume a steady flow perpendicular to the shock front and use a coordinate system fixed to the discontinuity. Denoting the preshocked or upstream gas as "u" and the postshocked or downstream gas as "d", we can write the mass, momentum and energy conservation laws as follows:

$$\rho_u v_u = \rho_d v_d, \tag{7.1}$$

$$\frac{1}{2}v_u^2 + w_u = \frac{1}{2}v_d^2 + w_d, \tag{7.2}$$

$$p_u + \rho_u v_u^2 = p_d + \rho_d v_d^2. \tag{7.3}$$

where v is the velocity of the fluid, p the pressure, ρ the density, $w \equiv \varepsilon + p/\rho$ the specific enthalpy (i.e. per unit mass), and ε the specific internal energy. The above equations are the well known Rankine-Hugoniot conditions for a stationary one-dimensional adiabatic flow. For more details on these equations the reader is referred to Ref.[4].

Notice that the Rankine-Hugoniot conditions involve three thermodynamic variables, i.e. ρ, p and w. Thus, we need to know the equation of state of the fluid in order to know the velocity and the thermodynamic state of the fluid on one side of the shock in terms of the variables on the other side. For simplicity we shall consider an ideal gas with polytropic index γ, for which we have

$$w = \frac{\gamma p}{(\gamma-1)\rho} = \frac{c_s^2}{(\gamma-1)}, \tag{7.4}$$

being c_s the velocity of sound. Defining the Mach number as $M \equiv v/c_s$ we easily obtain from Eqs. (7.1,7.2,7.3):

$$\frac{\rho_d}{\rho_u} = \frac{v_u}{v_d} = \frac{(\gamma+1)M_1^2}{(\gamma-1)M_1^2+2}. \tag{7.5}$$

In the limit of a strong adiabatic shock ($M_1 \to \infty$) we find an upper limit for the compression and the velocity ratio:

$$\frac{\rho_d}{\rho_u} = \frac{v_u}{v_d} = \frac{(\gamma+1)}{(\gamma-1)}, \tag{7.6}$$

which for $\gamma = 5/3$ reads:

$$\frac{\rho_d}{\rho_u} = \frac{v_u}{v_d} = 4. \tag{7.7}$$

8. First order Fermi mechanism

In 1978, Bell [12] and Blandford & Ostriker [13] proposed a first order acceleration mechanism occurring around shock waves. As mentioned before, numerical simulations show how

charged particles perform a random walk motion around a shock discontinuity due to scattering with magnetic inhomogeneities in the turbulent plasma (see Fig. 5). In a simplified one-dimensional picture we may consider that a relativistic particle traverses a shock front and is back-scattered many times on both sides of the shock (magnetic mirror effect). If we assume that the inhomogeneities are 'frozen' in the fluid, we can straightforwardly apply the expression obtained at the end of Section 6. When the cosmic ray is reflected in the upstream flow there is an energy gain $2v_u/c$. When it is reflected in the downstream flow there is an energy loss $2v_d/c$. But $v_u > v_d$, thus, in one "back and forth" cycle there is a net energy gain $\Delta E/E \propto 2(v_u - v_d)/c$. A more complete treatment, including variable scattering angles, leads to an energy gain per cycle given by:

$$\frac{\Delta E}{E} = \frac{4}{3}\frac{(v_u - v_d)}{c}. \tag{8.1}$$

In order to calculate the spectrum of the particles we can use the Fokker-Plank equation to describe the energization. Since this topic will be addressed in detail by P. Blasi in this Proceedings, we shall only present a simple argument showing that a power law spectrum is obtained [14]. Let us write the energy gain per cycle of a cosmic ray as a fraction of its energy, $\Delta E = \eta E$. After n cycles its energy will be $E = E_0(1+\eta)^n$, being E_0 the initial energy. Now, we can put the number of acceleration cycles as a function of the energy:

$$n = \frac{\ln(E/E_0)}{\ln(1+\eta)}. \tag{8.2}$$

Since the cosmic ray can escape from the shock region at any time, we shall define the probability P that the particle stays in the system for one more cycle. Thus, after n cycles the number of remaining cosmic rays is $N = N_0 P^n$, where N_0 is the initial number of particles. Substituting the expression for n obtained above we have:

$$N = N_0 P^{\frac{\ln(E/E_0)}{\ln(1+\eta)}}. \tag{8.3}$$

From the latter expression we obtain

$$\frac{N}{N_0} = \left(\frac{E}{E_0}\right)^{\frac{\ln P}{\ln(1+\eta)}}, \tag{8.4}$$

which is the number of cosmic rays with energy larger than E (i.e. with more that n cycles). Thus, the differential energy spectrum dN/dE follows a power law

$$\frac{dN}{dE} \propto E^{\frac{\ln P}{\ln(1+\eta)}-1}. \tag{8.5}$$

A more rigorous calculation (see e.g. P. Blasi in this Proceedings) allows to show that the exponent is $\sim 2-3$, i.e. in agreement with the observed values.

To finish, we emphasize that although the first order Fermi process is now recognized as the most important acceleration mechanism in astrophysical plasmas, various other mechanisms are relevant in specific applications. For a recent review the reader is referred to [15].

References

[1] see http://www.skatelescope.org/

[2] Proceedings of the Conference 'Magnetic fields in the universe: From Laboratory and Stars to Primordial Structures'; AIP Conf. Proc. Volume 784, pp. 253-262 (2005); Eds. E. M. de Gouveia Dal Pino, G. Lugones and A. Lazarian.

[3] R. Beck, AIP Conf. Proc., Volume 1085, pp. 83-96 (2008); in the Proceedings of the 4th International Meeting on High Energy Gamma-Ray Astronomy.

[4] L. D. Landau and E. M. Lifshitz, Fluid Mechanics, Volume 6 of Course of Theoretical Physics, Second Edition, Pergamon Press (1987); R. Courant and K. O. Friedrichs, Supersonic Flow and Shock Waves, Springer (1999); Ya. B. Zel'dovich and Yu. P. Raizer, Physics of Shock Waves and High-Temperature Hydrodynamic Phenomena, Academic Press (1966).

[5] E. Fermi, Phys. Rev., 75, 1169 (1949).

[6] F.C. Chen, Introduction to Plasma Physics and Controlled Fusion, Springer (2006).

[7] P. Goldreich, Peter and W. H. Julian, Astrophysical Journal, vol. 157, p.869 (1969).

[8] M. Vietri, Foundations of High-Energy Astrophysics, University of Chicago Press (2008).

[9] S. L. Shapiro and S. A. Teukolsky, Black holes, white dwarfs and neutron stars, Wiley (1983)

[10] J. Niemiec and M. Ostrowski, The Astrophysical Journal 610, 851Ű867 (2004).

[11] M. G. Baring and E. J. Summerlin, in Proc. of the 8th International Astrophysics Conference *Shock Waves in Space and Astrophysical Environments* (2010), eds. X. Ao, R. Burrows and G. P. Zank (AIP Conf. Proc., New York).

[12] A.R. Bell, Monthly Not. R. Astron. Soc., 182, 147 (1978).

[13] R.D. Blandford and J.P. Ostriker, Astrophys. J. Lett., 221, L29 (1978).

[14] D. H. Perkins, Particle Astrophysics, Oxford University Press (2009).

[15] D. B. Melrose, e-print arXiv:0902.1803.